Developmental Phases of Individual Mouse Preimplantation Embryos Characterized by Lipid Signatures using Desorption Electrospray Ionization Mass Spectrometry

Analytical Bioanalytical Chemistry, 404, 10, 2012, DOI 10.1007/s00216-012-6426-4

C.R. Ferreira, V. Pirro, L.S. Eberlin, J.E. Hallett, R.G. Cooks
Volume 404, Springer, 2012, 2915-2926

Abstract

Knowledge of the lipids present in individual preimplantation embryos is of interest in fundamental studies of embryology, in attempts to understand cellular pluripotency and in optimization of in vitro culture conditions necessary for the application and development of biotechnologies such as in vitro fertilization and transgenesis. In this work, the profiles of fatty acids and phospholipids (PL) in individual mouse preimplantation embryos and oocytes were acquired using an analytical strategy based on desorption electrospray ionization mass spectrometry (DESI-MS). The methodology avoids sample preparation and provides information on the lipids present in these microscopic structures. Differences in the lipid profiles observed for unfertilized oocytes, two- and four-cell embryos, and blastocysts were characterized. For a representative set of embryos (N= 114) using multivariate analysis (specifically principal component analysis) unfertilized oocytes showed a narrower range of PL species than did blastocysts. Two- and four-cell embryos showed a wide range of PLs compared with unfertilized oocytes and high abundances of fatty acids, indicating pronounced synthetic activity. The data suggest that the lipid changes observed in mouse preimplantation development reflect acquisition of a degree of cellular membrane functional and structural specialization by the blastocyst stage. It is also noteworthy that embryos cultured in vitro from the two-cell through the blastocyst stage have a more homogeneous lipid profile as compared with their in vivo-derived counterparts, which is ascribed to the restricted diversity of nutrients present in synthetic culture media. The DESI-MS data are interpreted from lipid biochemistry and previous reports on gene expression of diverse lipids known to be vital to early embryonic development.

Keywords

Desorption electrospray ionization . Lipid analysis . Embryology . Preimplantation development

Introduction

Oocyte fertilization in mammals occurs in the ampulla of the oviduct, close to the ovary. After this event, the embryo travels down the oviduct to the uterus taking 3 days in the case of the mouse. When the embryo reaches the uterus, usually at the blastocyst stage, the first events of cellular differentiation are observable. Preimplantation development, which can also occur in vitro, involves distinct metabolic phases, with radical changes in gene expression, protein synthesis, energy production, and metabolic requirements as the embryo develops from a fertilized zygote into a blastocyst [1].

Most research involving mammalian preimplantation embryo metabolism is based on studies of gene expression[2–5] and on the use of fluorescence microsco by using fluorescein isothiocyanate or similar fluorescent dyes to observe expressed proteins [6–8]. Lately, interest in addressing the chemical nature of lipids in these microscopic structures has increased, mainly based on results of lipid staining, gas chromatography (GC), and fatty acid (FA) supplementation during in vitro culture. These studies also showed that lipid metabolism is altered by in vitro culture conditions and that lipid cytoplasmic content seems to be crucial for oocyte and early embryo cryopreservation success [9–11]. FA metabolism occurs mostly in mitochondria, and it is poorly explored in early embryogenesis. The main FA breakdown pathway involves beta-oxidation in which FAs are degraded to acetyl-CoA fragments, which in their turn can be used as substrates for the mitochondrial Krebs cycle [12]. Inhibition of the beta-oxidation pathway by impairing the entry of activated FA into the mitochondria using the drug etomoxir (an inhibitor of carnitine palmitoyl tranferase I) decreases mouse oocyte maturation, zygote cleavage, and blastocyst development, suggesting that FAs are an important energy source in murine oocyte maturation and preimplantation development [13].

Phospholipids (PL), the major class of cellular lipids, constitute cell membranes and are involved in key cell signaling events [14, 15]. A 13-fold increase in phosphocholine (PCho) synthesis in mouse embryos from the two- to eight-cell stages has been previously reported by supplementing the culture medium with labeled choline (methyl-3H-choline) as a lipid precursor, suggesting not only membrane synthesis activity but also membrane remodeling during preimplantation development [16]. The enzyme cytidine 5′-triphosphate phosphocholine cytidylyltransferase, which participates in the biosynthesis of choline-containing PL, has been shown to be present in mouse oocyte and early embryo extracts using a specific enzymatic assay [17]. Also, a membrane choline transporter has been identified in the mouse embryo and it undergoes a 100-fold increase in concentration from the two-cell to the blastocyst stage [18]. FA and complex lipids have been detected in mouse, cattle, pig, sheep, and human embryo samples by colorimetric assays, thin-layer chromatography, or GC. These techniques rely on sample pooling (10–1,000 organisms) and lipid extraction and identification [11, 19–21]. Moreover, these methods give limited lipid structural information, typically

only information on the general lipid class or on fatty acyl residues. Advances in instrumentation and ionization methodologies in mass spectrometry (MS) allow FAs and glycerophospholipids to be detected as intact ionized molecules. MS can therefore be used to study the lipid composition of a broad range of samples of complex composition containing limited amounts (a few picograms) of lipids [22, 23]. Matrix-assisted desorption/ionization (MALDI), time-of flight secondary ion mass spectrometry (SIMS), and desorption electrospray ionization (DESI) have already been introduced as MS-based approaches for individual mammalian oocyte and embryo lipid analysis [24–27]. DESI is one of the ambient ionization MS strategies which allows sensitive detection and identification of free FA and intact species of glycerophospholipids [28]. In ambient ionization MS, ions are formed outside the mass spectrometer without sample preparation or separation in unmodified samples [29]. Addressing the chemical composition of microscopic samples such as individual organisms or small cell populations is a bioanalytical challenge which is being overcome by diverse MS ionization strategies, such as nanoESI, MALDI, SIMS, laser ablation electrospray ionization, and DESI [24, 30, 31]. For example, MS analysis and identification of microorganisms, mostly performed by commercial platforms based on MALDI, is revolutionizing the field of microbiology [30]. Similarly, using DESI, direct analysis of microorganisms showed that characteristic constituents of bacteria can be detected; in particular, acylium ions of FA are observable directly, not as the usual methyl ester derivatives [32, 33]. DESI allows rapid in situ analysis of samples in their native state and has been used to study the chemical composition of animal tissues, plants, and documents in an untargeted fashion [34]. DESI-MS is here applied to study the lipid composition of preimplantation mammalian embryos, with the aim of better understanding embryonic metabolic needs. This knowledge can be applied in diverse areas including the practical one of development of culture media that better mimic in vivo conditions. This could result in more successful cryopreservation and fetal development potential after embryo transfer to the maternal environment in artificial insemination or in embryo transfer programs. Lipid changes detected by DESI-MS observed in preimplantation mouse embryos are correlated with embryo biosynthetic activity and membrane structural and functional specialization. The lipid profile is used to monitor metabolic status of embryo development as well as to follow the impact of in vitro culture conditions. The observed differences in lipid profiles are integrated with existing information on upstream lipid metabolism in order to better understand the findings.

Materials and methods

This study was carried out in strict accordance with the Purdue animal care and use committee approved protocol (No. 1111000314). When not otherwise stated, reagents were purchase from Sigma-Aldrich (St. Louis, MO). Experimental design, sample collection, and preparation The experimental design included the use of two laboratory mouse lineages (BCB and FVB) in order to

evaluate if the lipid profiles were specific to a particular strain. Samples were obtained from BCB (C57BL/6×CBA) and FVB mouse strains breed at the Purdue University Center for Cancer Research's Transgenic Mouse Core Facility. Animals were superovulated at day 1 with 0.1 mL (5 IU) pregnant mare serumgonadotropin (i.p.) followed 46 h later by 0.1 mL (5 IU) human chorionic gonadotropin (i.p.) and were kept unmated (for unfertilized oocyte retrieval; N031) or were mated to allow oocyte fertilization. Some of the mice were euthanized 2 days after mating for two- (N018) and four-cell (N015) embryos retrieval and at 4 days after mating for in vivo derived blastocyst (N039) collection. Some two-cell embryos were cultured in vitro in potassium simplex optimized medium drops containing 30 μL for 2 days (in vitro blastocyst group; N011) at 37 °C and 5%CO2 in air. Sample preparation followed a previous report [24] and consisted of brief wash steps performed under a LEICA stereomicroscope using a finely pulled glass pipette. The oocytes and embryos were washed three times in groups of five structures (oocytes or embryos) in 20 μL containing drops of phosphate-buffered saline (PBS; Gibco BRL, Gaithersburg, MD)+0.1 % polyvinyl alcohol (PVA) in order to remove lipids present in the extracellular environment (flushing or culture medium). Another three washes were performed in 10 μL containing drops of methanol (Mallinckrodt Baker Inc, Phillipsburg, NJ)/ultrapure water 1:1 (v/v) in order to eliminate salts present in the PBS, which can interfere in the mass spectrometric analysis. Oocytes or embryos where then individually placed onto the surface of a glass slide (Gold Seal, Portsmouth, NH), which contained small circles drawn in the back with a permanent marker, in order to facilitate the identification and labeling of the samples. Samples were analyzed fresh or the glass slides were stored at −80 °C until analysis, when they were thawed and allowed to dry at room temperature for 15 min (Fig. 1a, b). Prior to DESI-MS analyses, the ink circles used to locate the embryos were blackened using a permanent marker in order to better visualize sample positions when directing the DESI spray (Fig. 1c). Mass spectrometric analysis by DESI A LTQ linear ion trap mass spectrometer (Thermo Fisher Scientific San Jose, CA) controlled by XCalibur 2.0 software and operated in the negative ion mode was used for the experiments. The instrument parameters were as follow: injection time, 500 ms; two micro scans; m/z range, 400–1,000; −50 V capillary voltage; and −25 V tube lens voltage. The DESI-MS analysis involves impacting the sample with charged droplets of a solvent. A thin layer of solvent is formed on the sample surface into which analytes dissolve. As other primary droplets arrive at the sample surface, they splash secondary micro droplets containing the dissolved analytes from the solvent film. This mechanism, droplet pickup" [35], causes analyte-containing droplets to be generated in the open air and then delivered to the mass spectrometer through a heated extended capillary. The DESI solvent combination used for the experiments was acetonitrile (ACN)+dimethylformamide (DMF) 1:1 (v/v) [36]. A spray voltage of 5 kV was applied to the stainless steel needle of a 250-μL glass syringe delivering solvent at a flow rate of 1.0 μL/min. The DESI spray nitrogen pressure was set at 180 psi, and the spray tip was positioned ~2 mm from the sample placed in a glass slide at an incident angle of 50°. DESI-MS

data were usually collected for 2–3 min/sample. Before analyzing the samples, mouse brain tissue and test samples were used for spray optimization (spray angle and distance to the metal capillary and sample surface) in order to obtain high quality mass spectra.

Lipid characterization

Lipid attribution of most abundant ions observed in the samples has been confirmed by high-resolution mass measurements acquired using an Orbitrap mass spectrometer (Exactive, Thermo Fisher Scientific, San Jose, CA). The instrument was operated in the negative ion mode with the same DESI spray and solvent settings used for the data collection with the LTQ mass spectrometer. The Orbitrap instrumental conditions were: maximum injection time, 1,000 ms; one micro scan; m/z range, 150–1,000; −60 V capillary voltage; and −145 V tube lens voltage. Molecular formula matching and error calculations were performed using the instrument software (Xcalibur v.1.0.1.03, Thermo Fisher Scientific San Jose, CA) and online search of lipids containing the calculated molecular formulae was carried out in the LIPID MAPS database [37]. Lipid attributions based on high-resolution mass measurements data are listed in Table 1 and examples of mass spectra obtained are shown in Fig. S1 in the Electronic supplementary material (ESM).

Principal component analysis

For each embryo, a list of m/z values and ion abundances from averaged mass spectra was imported into Matlab software 7.0 version (The MathWorks, Inc., Natick, MA) and multivariate data processing was performed using in-house routines. Before performing principal component analysis (PCA), the number of spectral variables was reduced (1:4) by a consecutive-window averaging algorithm. Then, normalization with respect to the total ion chronogram was performed in order to correct for instrumental variability. Neither background correction nor smoothing filters was applied. PCA was performed on category column-centered data, in order to investigate separately strain and the developmental stage effects.

Results

Representative mass spectra and most abundant lipid ions As previously observed for lipid analysis in individual mouse oocytes and preimplantation embryos [24], FA dimer signals predominate in the region of m/z 400–650 and glycerophospholipids in the m/z 700–1,000 range. Prominent FA dimers were mostly composed of palmitic, linoleic, arachidonic, and docosahexanoenic acids. Complex lipids were represented by phosphatidylcholines (such as the chlorinated adducts of PCho (34:1), m/z 794.3; PCho (36:2), m/z 820.5; and PCho (38:4), m/z 844.5), phosphatidylinositols (such as deprotonated PI (38:4) of m/z 885.5), phosphatidylethanolamines (such as deprotonated PE (38:3) of m/z 768.3), and

phosphatidylserines (such as deprotonated PS (38:4) of m/z 810.7). DESI-MS analysis was performed on unfertilized oocytes (N031), two- (N018) and four-cell embryos (N015), and blastocysts (N039). Representative mass spectra of each of the four developmental stages are depicted in Fig. 2, and lipid attributions of the most abundant lipid ions are shown in Table 1.As attributed by high mass resolution in this work and by MS/MS analysis in our previous report [24], PCho (34:1) is the most abundant lipid present in unfertilized mouse oocytes while blastocysts present a more complex PL content, with predominant PCho (34:1), PCho (36:2), and PCho (38:4) species. Two- and four-cell embryos show abundant FA dimers while PCho (34:1) is the predominant PL ion. DESI-MS of four other samples for each developmental stage are shown in Figs. S2, S3, S4, and S5 in the ESM. Note that despite the biological variability that is expected to occur in samples obtained from two different mouse strains and many individuals, similar trends in lipid profiles described for each developmental stage are observed.

DESI-MS extraction process

Time dependence of the DESI-MS was observed for most of these microscopic samples. For most of the samples analyzed, FA dimers were more abundantly detected in the first minute of the 2- to 3-min analysis period while the ion signal for PL predominated later (Fig. 3).

Effect of the mouse strain

PCA is commonly used for exploratory investigations of the complex information contained in a full mass spectral dataset, to allow consideration of all the spectral variables and their intercorrelations simultaneously [38]. As described elsewhere [39], the principal components (PCs) can be considered as orthogonal (i.e., uncorrelated) directions in the multidimensional data space that efficiently describe large fractions of the information. The projections of the data objects onto the PCs are called scores while the importance of each original variable in defining a certain PC is given by the loading coefficient. In the score plot, it is possible to visualize groupings that indicate similarities among objects on the basis of the information derived from the mass spectra, and these can be associated with particular characteristics of the samples analyzed. Subsequently, an examination of both the loading plot and the score plot allows chemical characterization of the studied samples to be achieved, revealing which m/z peaks are the most important in defining the sub-sets of samples under consideration. For statistical analysis of the effects of mouse strain, mass spectral data of all samples from both strains (FVB—N051 and BCB—N063) used were processed in order to eliminate any effect due to developmental stage. For the statistical data analysis, we have considered combinations of the three first three PCs (PC1, PC2, and PC3) in two-dimensional graphs to better visualize trends in experimental groupings. PCs are ranked in terms of the variance they explain and the first three PCs represent most of the information that was in the original datasets. For example, PC1+PC2+PC3 represented

74.3 % of the strain analysis dataset variance (Fig. 4a, b), but no evident clusters involving red (BCB) or dark blue (FVB) objects were observed. This indicates that there is no detectable effect of mouse strain on the lipid profiles in this test. Just a small trend of separation was observed in PC3, associated with the ion m/z 612.5 according to the loading plot (not shown). The other PC values (PC4 and PC5) also did not show clustering due to strain differences (data not shown). Based on these results, we disregarded embryo origin in performing developmental stage comparisons and consequently are able to draw conclusions that can be applied to mouse preimplantation development in general terms.

Differences in lipid signatures

With no clear effect of the mouse strain observed, category column centering was applied to the DESI-MS to follow the effects of the development stage by PCA. Differences in the lipid profiles that can be ascribed to the developmental stage were evident in the PC1 vs. PC3 (total of 52.1 % of the data variability) score plot (Fig. 5a). Two clusters are evidently represented by unfertilized oocytes and blastocysts, which are the most biologically distant phases of preimplantation development studied. Two- and four-cell embryos showed higher individual variability and the related objects in the score plot are more widely dispersed. (These data are consistent with visual inspection of the mass spectra shown in Fig. 2.). A trend towards separation among the samples is more evident in Fig. 5b where the centroid value for each category is depicted. The centroid value of unfertilized samples is situated closer to those of two- and four-cell embryos while the centroid value of the blastocyst is more distant. The ion m/z values which are relevant for samples' positioning in the PCA score plot can be observed in the loading plot (Fig. 5c). To interpret these data, Fig. 5a, c should be visualized together. The values of m/z showed in Fig. 5c, which are situated close to where the samples are located in Fig. 5a, are significant for the samples location in the PCA plot. Consistent with what has been observed in the representative mass spectra (Fig. 2), the most relevant ion for unfertilized oocyte clustering is the m/z 794 (PCho (34:1)+Cl)− (which contributes most to PC3 definition). Two- and four-cell embryos were both characterized by a set of ions of lower m/z value corresponding to the FA dimers (which contribute the most to PC1 definition), while blastocysts had a greater contribution of heavier ions (mainly m/z 820 and 844), which correspond to PCho species (PCho (36:2)+Cl)− and (PCho (38:4)+Cl)− with fatty acyl residues containing larger carbon chains and higher levels of unsaturation.

Impact of in vitro culture on the lipid signatures of blastocysts

The impact of in vitro culture was more specifically evaluated by comparing 19 blastocysts which were developed in vivo with 11 blastocysts of the FVB strain, cultured in vitro for 2 days (from the two-cell to the blastocyst stage). PCA was performed on these selected samples in order to evaluate differences in their spectral variability. Considering the first two lower-order PCs (PC1 and

PC2), it is evident from the score plot that blastocysts produced in vitro present a relatively homogeneous profile while there was a higher individual variability in blastocysts produced in vivo. The dispersion along PC2 is mainly due to the oleic acid dimer (m/z 563) while PCho species (PCho (36:2)+Cl)− and (PCho (38:4)+Cl)− (the most abundant ions in the mass spectra) are most heavily involved in defining PC1 (Fig. 6).

Discussion

As established for brain, kidney, bladder, liver, and germ cell, DESI-MS lipid profiles in tissue can be correlated with pathophysiological state [40]. In this work, based on the DESI-MS approach previously reported [24], we show that lipid profiles from individual mouse preimplantation embryos display marked changes during early development. Unfertilized oocytes, two- and four-cell embryos, and blastocysts were analyzed by DESI-MS in an unmodified condition (samples were simply washed). Two mouse strains were used and also the impact of in vitro culture was addressed by profiling blastocysts that have been maintained in vitro culture from the two-cell stage (2 days of culture). The data provided underscore several reasons why DESIMS is very useful in lipid research. Minimum or no sample handling is needed: samples are generally analyzed in their unmodified state [40]. Second, FAs and PL are readily ionized under ambient conditions by DESI-MS in the negative ion mode to give deprotonated molecules or chlorine adducts [24] and these small molecules (usually under 1,200 Da) fall in the optimal range for efficient ionization and extraction by DESI spray solvents [29]. Specifically for analysis of lipids in microscopic samples, the choice of appropriate DESI solvents yields adequate ion signals due to efficient lipid extraction [36]. The limitations of DESIMS for lipid analysis are related to the measurement of the relative amounts of small molecules, since the analysis is performed in a complex mixture, the possibility of bias in the measurement of relative amounts of lipids cannot be ignored. Nonetheless, relative signals in DESI show good agreement with LC-MS/MS data [41]. Biological applications of DESI-MS are rapidly growing, especially for cancer research [39, 42, 43], evaluation of lipid accumulation pathologies [44], the study of inflammatory responses [45], and botanical and microorganism analysis [46, 47]. In parallel, multivariate analyses (such as PCA) plus customized software is being developed for the exploration and automated modeling of lipid data to aid in biological interpretation of DESI-MS data [39, 48]. The DESI spray solvent extracts lipids from the samples in such a way that in most of the samples FA dimers are concentrated in the first minute of analysis while the signal for PL takes longer to appear and remains stable for longer. Strong temporal effects like this have not been observed in DESI-MS studies on tissue sections and may be related to peculiarities of embryos, perhaps as a result of the three dimensional shape of the samples or the presence of the zona pellucida, which may interfere with

the transport of lipids extracted from the sample. FA dimers occur frequently in DESI-MS analysis of biological samples and usually reflect the content of free FA in the samples [49].

Among chemometric techniques, either unsupervised or supervised analyses can be performed. The former, typified by PCA, mainly explore data variability and are used for visualizing and understanding the information encompassed in the experimental data [38, 39]. Application of this method to the present data revealed no evident effect of mouse strain (BCB vs. FVB) on the lipid profiles. This result was expected since mammalian preimplantation embryo development is a complex and highly conserved process, in which a number of correspondent genes have been observed in cross-species comparison of gene expression [50, 51]. Therefore, we believe that the lipid dynamics described herein will be valid for all mouse species and probably in general for mammalian preimplantation development. PCho can be detected either in the positive ion mode as sodiated and potassiated adduct ions in the negative ion mode as chlorine adducts [24, 52]. We have chosen the negative ion mode for the experiments since it was more sensitive under our conditions of analysis. The most abundant PCho species in unfertilized oocytes, two- and four-cell embryos, was the PCho (34:1). In blastocysts, PCho species containing higher numbers of carbons in the fatty acyl residues and higher degrees of unsaturation, such as PCho (36:2), PCho (38:4), and PCho (38:5), yielded the most abundant ions and were relevant for PCA clustering. Higher abundance PCho species containing 38 carbons with four or more units of unsaturation in the lipid profiles of blastocysts are indicative of the presence of arachidonic acid, which is needed for increased signaling activity in later preimplantation stages. Arachidonic acid is released from PL molecules by the enzyme phospholipase A2 and converted to eicosanoids, which have a number of cellular signaling functions [53]. Also, fatty acyl residues with higher unsaturation levels confer membrane fluidity, which indicates intense membrane signaling activity [54]. The PCho structures detected in the four developmental stages contain combinations of palmitic, stearic, oleic, linoleic and arachidonic as fatty acyl residues, which have been reported as the main fatty acyl residues detected by GC in domestic species (swine, sheep, bovine, and human) [19, 20, 55]. The high abundance of PCho adducts can be correlated with the fact that they represent more than 40 % of total cellular lipids and the major bilayer membrane structural lipid [53].

Limited information about lipid metabolism in preimplantation embryos is available: nevertheless, our data are consistent with research indicating that FA metabolism is highly active in mouse early development [10, 13, 21]. FA dimers were most abundant in two- and four-cell embryos, when maternal–zygotic transition has already occurred in the mouse species and the embryo genome is actively translated. This event in the mouse is reflected in numerous gene expression pathways related to the metabolic rate increase for synthetic activity needed for the cellular divisions [56].

The DESI-MS results can be also correlated upstream with reports on the gene expression of carnitine palmitoyl transferase I (CPT1B), an enzyme responsible for the internalization of FA in mitochondria, which was increased in mouse-unfertilized oocytes after ovulation and in blastocysts

and its inhibition and upregulation have had an impact in embryo development [13]. This enzyme has been studied in bovine preimplantation development using methyl palmoxirate to block the oxidation of FA. Similar results have been observed for the mouse species [57], so that the DESIMS findings on the changes in FA abundances could be related upstream in the embryo metabolism to the CPT1B enzymatic activity.

Phosphatidylethanolamine constitutes 20–30 % of the total cell PL. These lipid species are able to bind to proteins by hydrogen bounding through the primary amine in the polar headgroup, so that membrane stabilization is promoted [58]. PE species are readily detected by DESI in the negative ion mode as deprotonated species. The main PE species detected in the samples (PE (38:4) and PE (38:3)) have arachidic and arachidonic acid units in their structures. PE species have been reported as important lipids during early mouse pregnancy and have been colocalized with cyclooxygenase-2, which uses PL as substrates for cellular signaling process [59]. Nonetheless, we have not observed ion abundance changes in PE species during mouse preimplantation development, probably because implantation processes are still not significantly activated.

Phosphatidylinositols represent 10–15 % of the total cellular lipids and PI-derived compounds participate in diverse cellular pathways such as intracellular calcium signaling, gene transcription, RNA editing, nuclear export, and protein phosphorylation [60]. Usually, PI species are observed in small abundances in MS imaging of tissues [40, 61] and we have also observed small abundances of PI species throughout mouse preimplantation development. Changes in this lipid class have been observed latter in mouse embryo development (uterine implantation) and were related to the presence of angiogenic regions [59]. The impact of in vitro culture conditions (source of protein supplementation in the culture medium and oxygen concentration in the incubator) is well recognized and a focus of active research in embryology [62]. Changes in the lipid profile recorded by MALDI-MS have been reported for bovine preimplantation embryos produced in vitro but not compared to in vivo counterparts [25]. In the present work, fertilization and first cleavage in vivo and in vitro culture was performed over a period of 2 days, from the two-cell until the blastocyst stage. A more reproducible lipid profile was observed for the in vitro-cultured samples, probably due to nutrient restriction in the defined culture medium. We speculate that differences will be more evident comparing blastocysts which have been fertilized in vitro with in vivo-collected counterparts using DESI-MS. Also, with the use of higher spatial resolution DESI-MS imaging settings, which have recently allowed ~35μm feature definition in tissue samples [63], chemical screening of early embryos, especially of large domestic animals, may provide further information on lipid distributions in single embryos. In our study, the use of multivariate analyses was essential in order to support data interpretation of the large amount of information contained in the DESI-MS lipid profiles, so that informative changes on FA and glycerophospholipids during mouse preimplantation development could be evidenced. Lipid changes detected by DESI-MS indicate a pronounced FA metabolism in mouse two- and four-cell embryos and a functional and signaling

specialization of the cellular membranes in blastocysts. These findings have been supported by previous literature reports on lipid gene and protein expression in preimplantation embryos.

Acknowledgments

Support from the Purdue University Center for Cancer Research Small Grants is gratefully acknowledged. Additional support from NSF DBI-0852740 is also acknowledged. We thank Annemarie Kaufmann for technical assistance and Sean E. Humpfrey for discussion of the data.

References

1. Bavister BD (1998) Preimplantation embryo development (Serono Symposia USA). Springer, Berlin

2. Park CH, Uh KJ, Mulligan BP, Jeung EB, Hyun SH, Shin T, Ka H, Lee CK (2011) Analysis of imprinted gene expression in normal fertilized and uniparental preimplantation porcine embryos. PLoS One 6(7):e22216. doi:10.1371/journal.pone.0022216

3. Leidenfrost S, BoelhauveM, Reichenbach M, Gungor T, Reichenbach HD, Sinowatz F, Wolf E, Habermann FA (2011) Cell arrest and cell death in mammalian preimplantation development: lessons from the bovine model. PLoS One 6(7):e22121. doi:10.1371/journal.pone.0022121

4. Gal AB, Carnwath JW, Dinnyes A, Herrmann D, Niemann H, Wrenzycki C (2006) Comparison of real-time polymerase chain reaction and end-point polymerase chain reaction for the analysis of gene expression in preimplantation embryos. Reprod Fertil Dev 18(3):365–371

5. Niemann H, Wrenzycki C (2000) Alterations of expression of developmentally important genes in preimplantation bovine embryos by in vitro culture conditions: implications for subsequent development. Theriogenology 53(1):21–34

6. Fear JM, Hansen PJ (2011) Developmental changes in expression of genes involved in regulation of apoptosis in the bovine preimplantation embryo. Biol Reprod 84(1):43–51. doi:10.1095/biolreprod.110.086249

7. Hansis C, Edwards RG (2003) Cell differentiation in the preimplantation human embryo. Reprod Biomed Online 6(2):215–220 8. Schulz LC, Roberts RM (2011) Dynamic changes in leptin distribution in the progression from ovum to blastocyst of the preimplantation mouse embryo. Reproduction 141(6):767–777. doi:10.1530/REP-10-0532

9. McKeegan PJ, Sturmey RG (2012) The role of fatty acids in oocyte and early embryo development. Reprod Fert Develop 24 (1):59–67. doi:10.1071/Rd11907

10. Sutton-McDowall ML, Feil D, Robker RL, Thompson JG, Dunning KR (2012) Utilization of endogenous fatty acid stores for energy production in bovine preimplantation embryos. Theriogenology 77(8):1632–1641. doi:10.1016/j.theriogenology.2011.12.008

11. Lapa M, Marques CC, Alves SP, Vasques MI, Baptista MC, Carvalhais I, Pereira MS, Horta AEM, Bessa RJB, Pereira RM (2011) Effect of trans-10 cis-12 conjugated linoleic acid on bovine

oocyte competence and fatty acid composition. Reprod Domest Anim 46(5):904–910. doi:10.1111/j.1439-0531.2011.01762.x
12. Michael I, Gurr JLH, Frayn KN (eds) (2005) Lipid biochemistry, 5th edn. Blackwell, Oxford
13. Dunning KR, Cashman K, Russell DL, Thompson JG, Norman RJ, Robker RL (2010) Beta-oxidation is essential for mouse oocyte developmental competence and early embryo development. Biol Reprod 83(6):909–918. doi:10.1095/biolreprod.110.084145
14. Fadeel B, Xue D (2009) The ins and outs of phospholipid asymmetry in the plasma membrane: roles in health and disease. Crit Rev Biochem Mol Biol 44(5):264–277. doi:10.1080/10409230903193307
15. Cazzolli R, Shemon AN, Fang MQ, Hughes WE (2006) Phospholipid signalling through phospholipase D and phosphatidic acid. IUBMB Life 58(8):457–461. doi:10.1080/15216540600871142
16. Pratt HP (1980) Phospholipid synthesis in the preimplantation mouse embryo. J Reprod Fertil 58(1):237–248
17. Moon EA, ONeill C (1997) CTP:phosphocholine cytidylyltransferase activity in the preimplantation mouse embryo. J Reprod Fertil 110(2):213–218
18. Vanwinkle LJ, Campione AL, Mann DF, Wasserlauf HG (1993) The cation receptor subsite of the choline transporter in preimplantation mouse conceptuses resembles a cation receptor subsite of several amino-acid transporters. Biochimica Et Biophysica Acta 1146(1):38–44
19. Kim JY, Kinoshita M, Ohnishi M, Fukui Y (2001) Lipid and fatty acid analysis of fresh and frozen-thawed immature and in vitro matured bovine oocytes. Reproduction 122(1):131–138
20. Matorras R, Ruiz JI, Mendoza R, Ruiz N, Sanjurjo P, Rodriguez-Escudero FJ (1998) Fatty acid composition of fertilization-failed human oocytes. Hum Reprod 13(8):2227–2230
21. Hillman N, Flynn TJ (1980) The metabolism of exogenous fatty acids by preimplantation mouse embryos developing in vitro. J Embryol Exp Morphol 56:157–168
22. Zhou M, Veenstra T (2008) Mass spectrometry: m/z 1983-2008. Biotechniques 44(5):667–668, 670. doi:10.2144/000112791
23. Casado B, Affolter M, Kussmann M (2009) OMICS-rooted studies of milk proteins, oligosaccharides and lipids. J Proteomics 73 (2):196–208. doi:10.1016/j.jprot.2009.09.018
24. Ferreira CR, Eberlin LS, Hallett JE, Cooks RG (2012) Single oocyte and single embryo lipid analysis by desorption electrospray ionization mass spectrometry. J Mass Spectrom 47(1):29–33. doi:10.1002/jms.2022
25. Ferreira CR, Saraiva SA, Catharino RR, Garcia JS, Gozzo FC, Sanvido GB, Santos LF, Lo Turco EG, Pontes JH, Basso AC, Bertolla RP, Sartori R, Guardieiro MM, Perecin F, Meirelles FV, Sangalli JR, Eberlin MN (2010) Single embryo and oocyte lipid fingerprinting by mass spectrometry. J Lipid Res 51(5):1218–1227. doi:10.1194/jlr.D001768

26. Fletcher JS, Lockyer NP, Vaidyanathan S, Vickerman JC (2007) TOF-SIMS 3D biomolecular imaging of Xenopus laevis oocytes using buckminsterfullerene (C60) primary ions. Anal Chem 79 (6):2199–2206. doi:10.1021/ac061370u
27. Kurczy ME, Piehowsky PD, Willingham D, Molyneaux KA, Heien ML, Winograd N, Ewing AG (2010) Nanotome cluster bombardment to recover spatial chemistry after preparation of biological samples for SIMS imaging. J Am Soc Mass Spectrom 21(5):833–836. doi:10.1016/j.jasms.2010.01.014
28. Manicke NE, Wiseman JM, Ifa DR, Cooks RG (2008) Desorption electrospray ionization (DESI) mass spectrometry and tandem mass spectrometry (MS/MS) of phospholipids and sphingolipids: ionization, adduct formation, and fragmentation. J Am Soc Mass Spectrom 19(4):531–543. doi:10.1016/j.jasms.2007.12.003
29. Cooks RG, Ouyang Z, Takats Z, Wiseman JM (2006) Detection technologies. Ambient mass spectrometry. Science 311 (5767):1566–1570. doi:10.1126/science.1119426
30. Drake RR, Boggs SR, Drake SK (2011) Pathogen identification using mass spectrometry in the clinical microbiology laboratory. J Mass Spectrom 46(12):1223–1232. doi:10.1002/jms.2008
31. Amantonico A, Urban PL, Zenobi R (2010)Analytical techniques for single-cell metabolomics: state of the art and trends. Anal Bioanal Chem 398(6):2493–2504. doi:10.1007/s00216-010-3850-1
32. Song Y, Talaty N, Tao WA, Pan Z, Cooks RG (2007) Rapid ambient mass spectrometric profiling of intact, untreated bacteria using desorption electrospray ionization. Chem Commun (Camb) 1:61–63. doi:10.1039/b615724f
33. Meetani MA, Shin YS, Zhang S, Mayer R, Basile F (2007) Desorption electrospray ionization mass spectrometry of intact bacteria. J Mass Spectrom 42(9):1186–1193. doi:10.1002/jms.1250
34. Nemes P, Vertes A (2012) Ambient mass spectrometry for in vivo local analysis and in situ molecular tissue imaging. TrAC Trends Anal Chem 34:22–34. doi:10.1016/j.trac.2011.11.006
35. Costa AB, Cooks RG (2007) Simulation of atmospheric transport and droplet-thin film collisions in desorption electrospray ionization. Chem Commun (Camb) 38:3915–3917. doi:10.1039/b710511h
36. Eberlin LS, Ferreira CR, Dill AL, Ifa DR, Cheng L, Cooks RG (2011) Nondestructive, histologically compatible tissue imaging by desorption electrospray ionization mass spectrometry. Chembiochem 12(14):2129–2132. doi:10.1002/cbic.201100411
37. Fahy E, Sud M, Cotter D, Subramaniam S (2007) LIPID MAPS online tools for lipid research. Nucleic Acids Res 35(Web Server issue):W606–W612, 10.1093/nar/gkm324
38. Jolliffe IT (2002) Principal component analysis. Springer Series in Statistics, 2nd edn. Springer, New York
39. Pirro V, Eberlin LS, Oliveri P, Cooks RG (2012) Interactive hyperspectral approach for exploring and interpreting DESI-MS images of cancerous and normal tissue sections. Analyst 137(10):2374–2380. doi:10.1039/c2an35122f

40. Eberlin LS, Ferreira CR, Dill AL, Ifa DR, Cooks RG (2011) Desorption electrospray ionization mass spectrometry for lipid characterization and biological tissue imaging. Biochim Biophys Acta 1811(11):946–960. doi:10.1016/j.bbalip. 2011.05.006
41. Wiseman JM, Ifa DR, Zhu Y, Kissinger CB, Manicke NE, Kissinger PT, Cooks RG (2008) Desorption electrospray ionization mass spectrometry: imaging drugs and metabolites in tissues. Proc Natl Acad Sci USA 105(47):18120–18125. doi:10.1073/pnas.0801066105
42. Eberlin LS, Norton I, Dill AL, Golby AJ, Ligon KL, Santagata S, Cooks RG, Agar NY (2012) Classifying human brain tumors by lipid imaging with mass spectrometry. Cancer Res 72(3):645–654. doi:10.1158/0008-5472.CAN-11-2465
43. Dill AL, Eberlin LS, Costa AB, Zheng C, Ifa DR, Cheng L, Masterson TA, Koch MO, Vitek O, Cooks RG (2011) Multivariate statistical identification of human bladder carcinomas using ambient ionization imaging mass spectrometry. Chemistry 17 (10):2897–2902. doi:10.1002/chem.201001692
44. Manicke NE, Nefliu M, Wu C, Woods JW, Reiser V, Hendrickson RC, Cooks RG (2009) Imaging of lipids in atheroma by desorption electrospray ionization mass spectrometry. Anal Chem 81 (21):8702–8707. doi:10.1021/ac901739s
45. Girod M, Shi Y, Cheng JX, Cooks RG (2011) Mapping lipid alterations in traumatically injured rat spinal cord by desorption electrospray ionization imaging mass spectrometry. Anal Chem 83 (1):207–215. doi:10.1021/ac102264z
46. Muller T, Oradu S, Ifa DR, Cooks RG, Krautler B (2011) Direct plant tissue analysis and imprint imaging by desorption electrospray ionization mass spectrometry. Anal Chem 83(14):5754–5761. doi:10.1021/ac201123t
47. Song Y, Talaty N, Datsenko K, Wanner BL, Cooks RG (2009) In vivo recognition of Bacillus subtilis by desorption electrospray ionization mass spectrometry (DESI-MS). Analyst 134(5):838–841. doi:10.1039/b900069k
48. Xiong X, Xu W, Eberlin LS, Wiseman JM, Fang X, Jiang Y, Huang Z, Zhang Y, Cooks RG, Ouyang Z (2012) Data processing for 3D mass spectrometry imaging. J Am Soc Mass Spectrom 23 (6):1147–1156. doi:10.1007/s13361-012-0361-7
49. Dill AL, Eberlin LS, Costa AB, Ifa DR, Cooks RG (2011) Data quality in tissue analysis using desorption electrospray ionization. Anal Bioanal Chem 401(6):1949–1961. doi:10.1007/s00216-011-5249-z
50. Adjaye J, Herwig R, Brink TC, Herrmann D, Greber B, Sudheer S, Groth D, Carnwath JW, Lehrach H, Niemann H (2007) Conserved molecular portraits of bovine and human blastocysts as a consequence of the transition from maternal to embryonic control of gene expression. Physiol Genomics 31(2):315–327
51. Vallee M, Aiba K, Piao Y, Palin MF, Ko MSH, Sirard MA (2008) Comparative analysis of oocyte transcript profiles reveals a high degree of conservation among species. Reproduction 135(4):439–

448. doi:10.1530/Rep-07-0342
52. Dill AL, Ifa DR, Manicke NE, Costa AB, Ramos-Vara JA, Knapp DW, Cooks RG (2009) Lipid profiles of canine invasive transitional cell carcinoma of the urinary bladder and adjacent normal tissue by desorption electrospray ionization imaging mass spectrometry. Anal Chem 81(21):8758–8764. doi:10.1021/ac901028b
53. Billah MM, Anthes JC (1990) The regulation and cellular functions of phosphatidylcholine hydrolysis. Biochem J 269(2):281–291
54. Helmreich EJ (2003) Environmental influences on signal transduction throughmembranes: a retrospectivemini-review. Biophys Chem 100(1–3):519–534
55. Lapa M, Marques CC, Alves SP, Vasques MI, Baptista MC, Carvalhais I, Silva Pereira M, Horta AE, Bessa RJ, Pereira RM (2011) Effect of trans-10 cis-12 conjugated linoleic acid on bovine oocyte competence and fatty acid composition. Reprod Domest Anim 46(5):904–910. doi:10.1111/j.1439-0531.2011.01762.x
56. Wang QT, Piotrowska K, Ciemerych MA, Milenkovic L, Scott MP, Davis RW, Zernicka-Goetz M (2004) A genome-wide study of gene activity reveals developmental signaling pathways in the preimplantation mouse embryo. Dev Cell 6(1):133–144
57. Ferguson EM, Leese HJ (2006) A potential role for triglyceride as an energy source during bovine oocyte maturation and early embryo development. Mol Reprod Dev 73(9):1195–1201. doi:10.1002/Mrd.20494
58. Dowhan W (1997) Molecular basis for membrane phospholipid diversity: why are there so many lipids? Annu Rev Biochem 66:199–232. doi:10.1146/annurev.biochem.66.1.199
59. Burnum KE, Cornett DS, Puolitaival SM, Milne SB, Myers DS, Tranguch S, Brown HA, Dey SK, Caprioli RM (2009) Spatial and temporal alterations of phospholipids determined by mass spectrometry during mouse embryo implantation. J Lipid Res 50 (11):2290–2298. doi:10.1194/jlr.M900100-JLR200
60. Di Paolo G, De Camilli P (2006) Phosphoinositides in cell regulation and membrane dynamics. Nature 443(7112):651–657. doi:10.1038/nature05185
61. Berry KA, Hankin JA, Barkley RM, Spraggins JM, Caprioli RM, Murphy RC (2011) MALDI imaging of lipid biochemistry in tissues by mass spectrometry. Chem Rev 111(10):6491–6512. doi:10.1021/cr200280p
62. Krisher RL, Wheeler MB (2010) Towards the use of microfluidics for individual embryo culture. Reprod Fertil Dev 22(1):32–39. doi:10.1071/RD09219
63. Campbell DI, Ferreira CR, Eberlin LS, Cooks RG (2012) Improved spatial resolution in the imaging of biological tissue using desorption electrospray ionization. Anal Bioanal Chem. doi:10.1007/s00216-012-6173-6

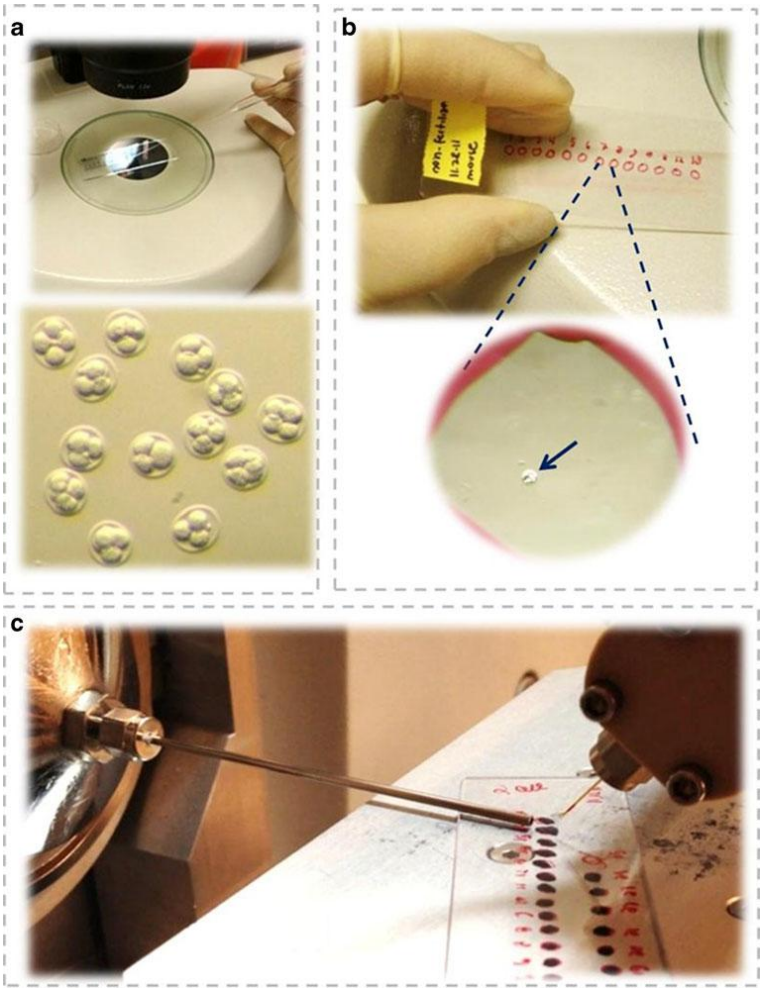

Fig. 1 Overview of sample handling for DESI-MS analysis of individual oocytes/preimplantation mouse embryos. **a** Samples washed under a stereomicroscope in PBS+0.1 % PVA and in methanol/water 1:1 (v/v) and **b** individually placed on glass slides. Arrow shows one embryo (~100 µm diameter) inside a red ink circle drawn in the back of the slide. **c** Lipid profiles recorded by DESI-MS by placing oocytes and embryos under the DESI spray spot. Optical imaging during the experiment shows the DESI spray tip directed towards the glass surface as well as the metal capillary used to conduct the ions to the mass spectrometer.

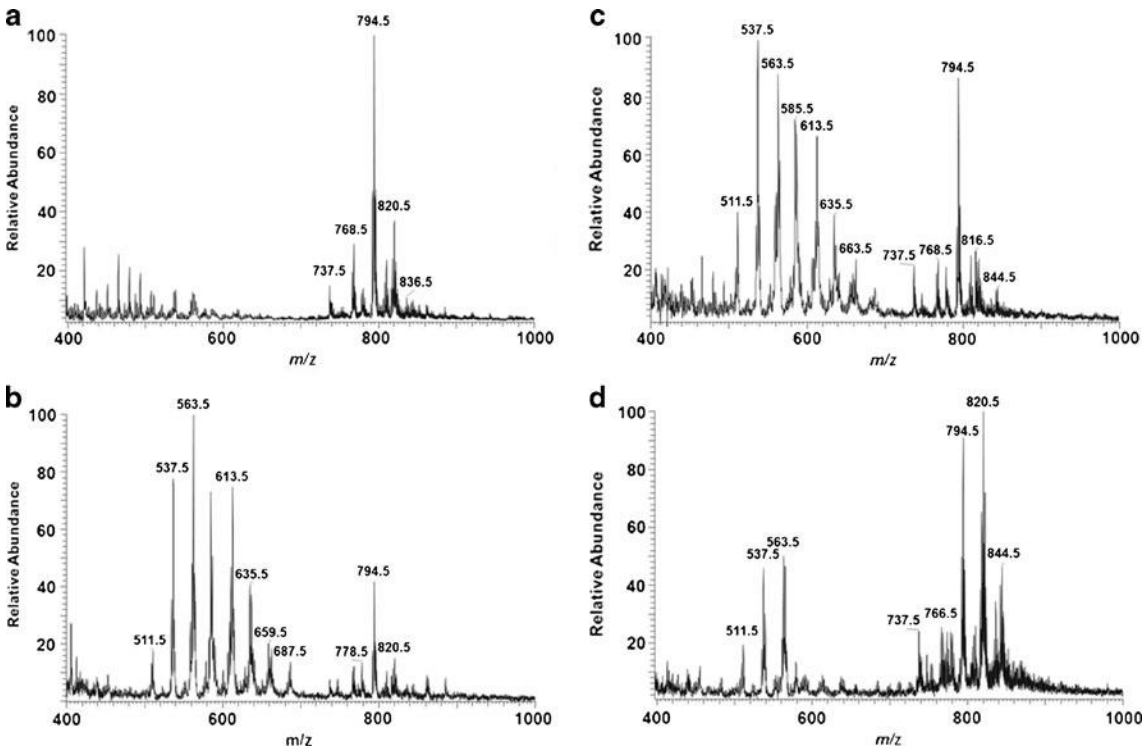

Fig. 2 Representative DESI-MS negative ion mode mass spectra (accumulated over 2–3 min of analysis for each sample) of individual oocytes and embryos from each of four mouse preimplantation developmental stages a unfertilized oocyte, b two-cell embryo, c four-cell embryo, and d blastocyst

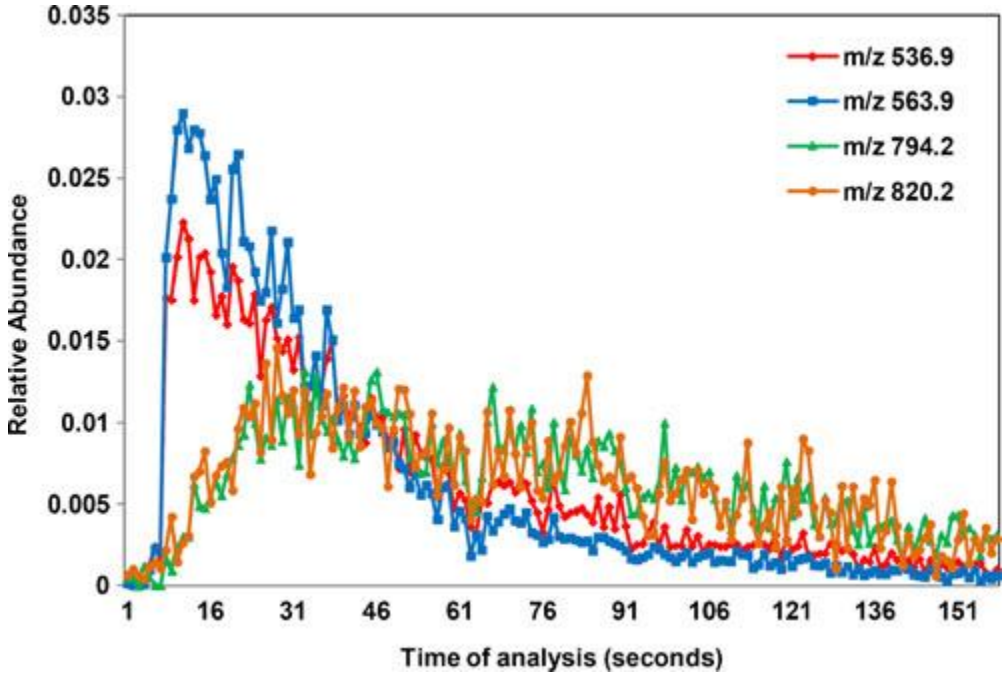

Fig. 3 Relative ion abundance vs. analysis time for two FA dimers (m/ z 536.9 and 563.9) and two PL species (m/z 794.2 and 820.2) present in a single unfertilized mouse oocyte. In the first minute of analysis, FA dimers are rapidly extracted from the sample by the ACN/DMF spray. Later, ion signals for PL species predominate

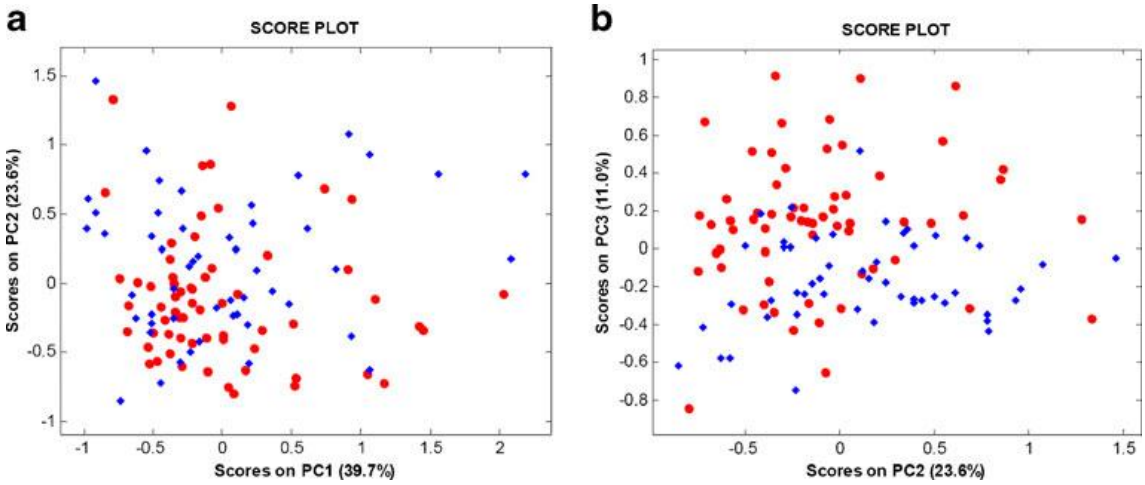

Fig. 4 PCA score plots generated to evaluate mouse strain effects (BCB and FVB strain tagged in red circles and blue diamonds, respectively). Graphs depicting a PC1 (39.7 % of data variability) vs. PC2 (23.9 % of data variability) and b PC2 vs. PC3 (11.0 % of data variability) show no evident effect of mouse strain on the lipid profiles

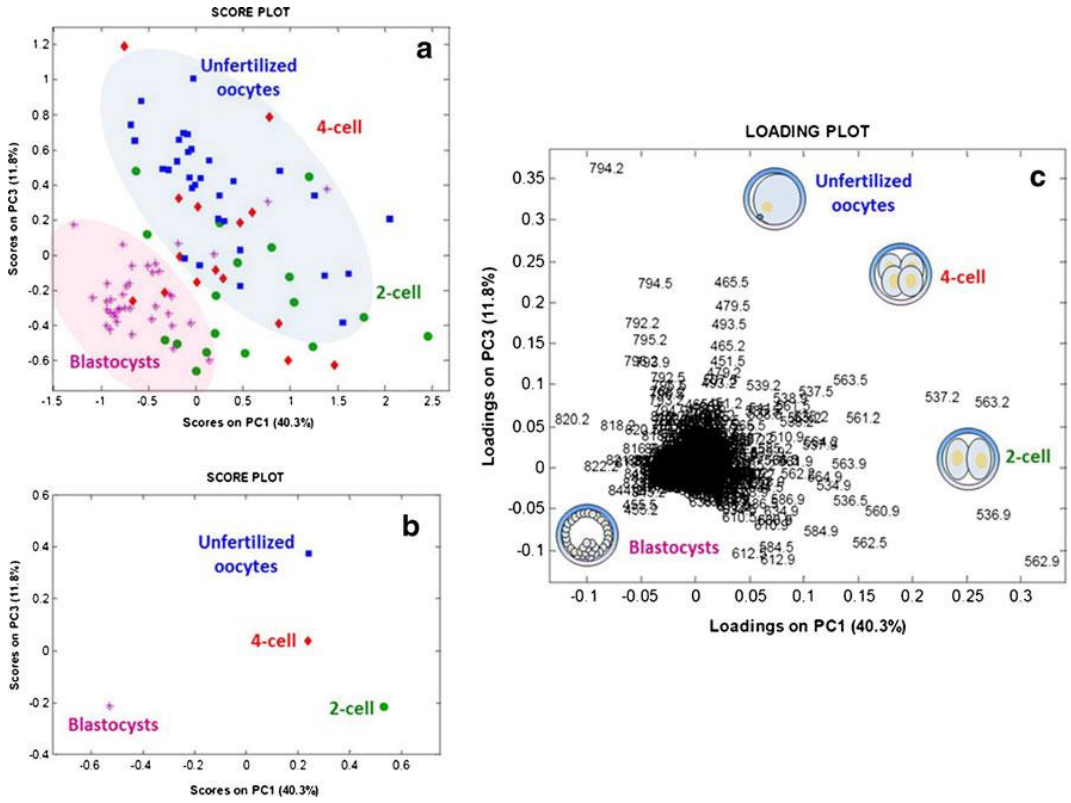

Fig. 5 a PCA score plot showing the distribution of unfertilized oocytes (blue squares), two- (green circles) and four-cell embryos (red diamonds), and blastocyst individuals (purple crosses). b PCA score plot showing the centroid value for each category of developmental stage depicted with the same color code; c PCA loading plot with the m/z values that contribute most to the distinctive positions of samples in the score plot

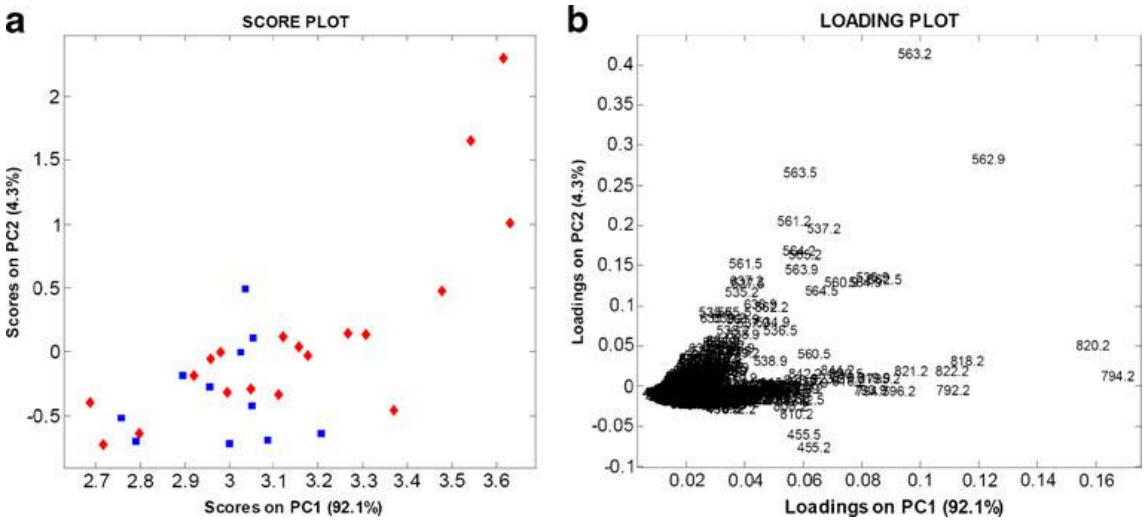

Fig. 6 PCA score (a) and corresponding loading (b) plot comparing DESI-MS lipid profiles of FVB blastocysts that have developed in vivo (red diamonds) with counterparts that have been maintained for 2 days in in vitro culture (blue squares). The tighter clustering of the in vitro samples corresponds to a more homogeneous lipid profile for the individual samples

Table 1 Abundant lipid ions observed in mouse preimplantation embryos analyzed in the negative ion mode and attributed by high-resolution mass spectrometry

Ion	Ion molecular formula	Delta ppm[a]	Attribution[b]
511.4727	$C_{32}H_{63}O_4$	0.663	16:0/16:0[c]
537.4880	$C_{34}H_{65}O_4$	0.243	16:0/18:1[c]
563.5042	$C_{36}H_{67}O_4$	1.003	18:0/18:2, 18:1/18:1, and 18:0/18:2[c]
585.4906	$C_{38}H_{65}O_4$	2.873	16:0/22:5, 18:2/20:3, 18:1/20:4, and 18:0/20:5[c]
613.5239	$C_{40}H_{69}O_4$	4.913	18:1/22:4, 18:0/22:5, 20:0/20:5, and 20:4/20:1[c]
747.5181	$C_{40}H_{76}O_{10}P$	−0.038	$(PG(34:1))^-$
766.5422	$C_{43}H_{78}NO_8P$	3.903	$(PE(38:4))^-$
768.5444	$C_{43}H_{80}NO_8P$	−9.391	$(PE(38:3))^-$
773.5337	$C_{42}H_{78}O_{10}P$	−0.128	$(PG(36:2))^-$
792.5295	$C_{42}H_{80}NO_8PCl$	−2.544	$(PC(34:2)+Cl)^-$
794.5479	$C_{42}H_{82}NO_8PCl$	0.848	$(PC(34:1)+Cl)^-$
810.5275	$C_{44}H_{77}NO_{10}P$	−1.946	$(PS(38:4))^-$
818.5440	$C_{44}H_{82}NO_8PCl$	−3.965	$(PC(36:3)+Cl)^-$
820.5629	$C_{44}H_{84}NO_8PCl$	0.115	$(PC(36:2)+Cl)^-$
844.5675	$C_{46}H_{84}NO_8PCl$	5.451	$(PC(38:4)+Cl)^-$
846.5761	$C_{46}H_{86}NO_8PCl$	−2.795	$(PC(38:3)+Cl)^-$
863.5646	$C_{45}H_{84}O_{13}P$	−1.080	$(PI(36:1))^-$
885.5495	$C_{47}H_{82}O_{13}P$	−0.443	$(PI\ (38:4))^-$

PG phosphatidylglycerol, *PE* phosphatidylethanolamine, *PC* phosphatidylcholine, *PS* phosphatidylserine, *PI* phosphatidylinositol

[a] High-resolution mass spectra were obtained from mouse unfertilized oocytes, two-cell embryos, and blastocysts. The Delta parts-per-million (ppm) column displays the difference between the specified mass and the calculated mass in parts per million

[b] Isomeric lipid species (possible fatty acyl residues combinations and positions of double bounds) cannot be determined by high-resolution mass spectrometry. Assignments are based on our previously recorded MS/MS data and literature reports [24, 32] and therefore are tentative

[c] Fatty acid dimer combinations have been tentatively assigned since dimers are not efficiently isolated for MS/MS experiments. Fatty acids trivial names: palmitic acid (16:0), stearic acid (18:0), oleic acid (18:1), linoleic acid (18:2), gadolenic or gondonic acid (20:1), dihomo gama linoleic or meadic acid (20:3), arachidonic acid (20:4), eicosapentaenoic acid (EPA; 20:5), docosatetraenoic (22:4), docosapentaenoic (DPA; 22:5)